HHS Public Access

Author manuscript

Nat Neurosci. Author manuscript; available in PMC 2015 July 01.

Published in final edited form as:

Nat Neurosci. 2015 January ; 18(1): 97–103. doi:10.1038/nn.3878.

COLUMNAR ORGANIZATION OF SPATIAL PHASE IN VISUAL CORTEX

Yushi Wang[*], **Jianzhong Jin**[*], **Jens Kremkow**, **Reza Lashgari**, **Stanley J. Komban**, and **Jose M. Alonso**

Graduate Center for Vision Research, State University of New York, College of Optometry, 33 West 42nd Street, New York, NY 10036, USA

Abstract

Images are processed in the primary visual cortex by neurons that encode different stimulus orientations and spatial phases. In primates and carnivores, neighboring cortical neurons share similar orientation preferences but spatial phases were thought to be randomly distributed. Here we reveal a columnar organization for spatial phase in cats that shares resemblances with the columnar organization for orientation. For both orientation and phase, the mean difference across vertically aligned neurons was less than 1/4 of a cycle. Cortical neurons showed three times more diversity in phase than orientation preference, however, the average phase of local neuronal populations was similar through the depth of layer 4. We conclude that columnar organization for visual space is not only defined by the spatial location of the stimulus but also by absolute phase. Taken together with previous studies, our results suggest that this phase-visuotopy is responsible for the emergence of orientation maps.

Neurons that are vertically aligned in visual cortex have receptive fields also aligned in visual space. This visuotopic organization (position in visual space), also called retinotopy (position in retinal space), is present in all mammals from mice to primates and is equivalent to the topographic map of body surface in the somatosensory cortex[1]. It is currently believed that the visuotopic organization of visual cortex does not take into account the contrast polarity of the stimulus (dark or light). That is, the receptive fields of neighboring cortical neurons are aligned in visual space but the spatial location of the receptive fields subregions that respond to light (ON) and dark stimuli (OFF) can be misaligned (Fig. 1a, left). The ON and OFF subregions are frequently described as the positive and negative phases of a sinusoid, therefore, cells that have their strongest OFF (or ON) subregions in the same position of visual space also have the same spatial phase (Fig. 1a, right). While a large body of work[2–5], including our own[6], has demonstrated phase misalignments between neighboring cortical neurons, a recent study found a robust phase bias in the population receptive field of thalamic afferents feeding the same cortical orientation column[7]. The main

Send correspondence to: Jose-Manuel Alonso, SUNY Optometry, Department of Visual Sciences, 33 West, 42nd street, 17th floor, New York, NY 10036, Voice: 212-938-5573, Fax: 212-938-5796, jalonso@sunyopt.edu.

[*]These two authors contributed equally to this work

Present address for Reza Lashgari: School of Electrical Engineering, Iran University of Science and Technology, Narmak, Tehran, Iran

prediction from this recent study is that the average spatial phase should remain constant through the depth of layer 4 (Fig. 1a, right), even if it varies among the individual neurons contributing to the average. Here, we tested this prediction by performing vertical electrode penetrations through layer 4 of cat visual cortex with a 16-channel silicon probe (Fig. 1b). Receptive fields were mapped by spike-trigger averaging the stimulus (binary white noise or gratings) and orientation/direction selectivity was measured with dark and light moving bars (Fig. 1c).

RESULTS

We found that the receptive fields of vertically aligned neurons were frequently dominated by the same contrast polarity, ON or OFF. The contrast polarity was calculated as the difference between the maximum response to light (ON) and dark (OFF) divided by the sum (contrast polarity = (ON−OFF)/(ON+OFF)). Cells that responded only to dark stimuli had a contrast polarity of −1 (OFF-dominated), those that responded only to light stimuli had a contrast polarity of +1 (ON-dominated) and those that responded equally to both had a contrast polarity of 0 (ON-OFF balanced). Our results demonstrate the existence of OFF dominated columns, in which OFF responses are stronger than ON responses through the depth of the cortex (Fig. 2a, left) and ON dominated columns, in which ON responses are stronger (Fig. 2a, right). In addition to the columnar organization for ON/OFF dominance, we demonstrate a columnar organization for absolute spatial phase. That is, the position and contrast polarity of the strongest subregion (spatial phase) does not vary randomly through the depth of the cortex as was previously thought (Figure 1a, left) but it remains constant (Figure 1a, right; Figure 2a). In some fortuitous experiments, we recorded from the ~ 100 micron transition between OFF and ON dominated columns (Fig. 2a, middle) and found occasional jumps in retinotopy through the horizontal dimension of layer 4 (Fig. 2a, middle), as reported previously[8]. However, the ON and OFF retinotopy was remarkably similar through the vertical dimension.

Columnar organization for ON/OFF dominance

To quantify the columnar organization for ON/OFF dominance, we made vertical multielectrode penetrations within layer 4, and mapped the receptive fields of neurons recorded in contiguous electrodes with white noise. Each penetration (n = 196) was classified as ON-dominated or OFF-dominated if all the contiguous receptive fields had the same contrast polarity (ON or OFF) and was counted only once (e.g. penetrations sampling 0.2 mm of layer 4 did not include sections of penetrations sampling 0.3 mm or 0.4 mm). We then calculated the percentage of vertical penetrations within layer 4 with receptive fields in contiguous electrodes that were all OFF-dominated (OFF domain), all ON-dominated (ON-domain) or mixed (ON/OFF mixed) and obtained the standard deviation of these percentages by bootstrapping (Fig. 2b, see online methods). The measured percentages of OFF domains (40%) and ON domains (20%) were higher than what it would be expected by chance, either if we assumed that OFF-dominated neurons were twice as frequent as ON-dominated neurons (Figure 2b, black bars) or if we assumed that OFF- and ON-dominated neurons were equally frequent (Figure 2b, gray bars; $P < 0.001$, Bootstrap, see online methods for details). Notice that the examples illustrated in Figure 2a are by themselves a

strong demonstration that OFF and ON-dominated columns are unlikely to be found by chance. For example, if we assume that there are two times more OFF-dominated than ON-dominated neurons in the cortex, the probability of finding 20 receptive fields that are all OFF dominated by chance in a group of neighboring vertical penetrations (the example shown in Figure 2a, left) would be $(2/3)^{20} = 3 * 10^{-4}$. Taken together, these results demonstrate the existence of vertical columns for ON and OFF dominance and indicate that OFF-dominated columns occupy two times more cortical space than ON-dominated columns in cat visual cortex (40% vs. 20% in Fig. 2b).

To measure the horizontal spread of ON and OFF dominated columns, we performed horizontal penetrations through cortical layer 4. These experiments also demonstrated that OFF-dominated columns spread over larger horizontal distances than ON-dominated columns (Fig. 2c, 0.36 versus 0.28 mm, $P = 0.002$, Bootstrap, see online methods for details), a finding that is consistent with the presumed larger horizontal spread for OFF than ON thalamic afferents in cat visual cortex[7]. The larger spread of OFF- than ON-domains was demonstrated with two different methods. In the first method, we counted the number of ON- and OFF-domains measured in horizontal penetrations as a function of the domain horizontal length (Figure 2c; we defined a horizontal domain as ≥ 3 receptive fields with the same contrast polarity in contiguous electrodes separated by 100 microns horizontally). This method frequently revealed OFF-domains with 0.5 mm of horizontal length (6 contiguous OFF-dominated receptive fields), however, ON-domains rarely spread more than 0.4 mm (Fig. 2c). In the second method, we obtained a normalized measure of the horizontal extent of ON and OFF domains by performing an ON/OFF-border trigger-average. We took all horizontal penetrations, assigned 1 to ON-dominated receptive fields and −1 to OFF dominated receptive fields and used the ON-OFF border as a trigger to average all horizontal penetrations (see online methods for details). The results from the ON/OFF-border trigger-average also indicate that OFF-domains spread over larger horizontal distances than ON-domains (Figure 2c, inset).

ON and OFF cortical domains driven by contralateral and ipsilateral eyes

To further quantify the difference in the cortical representation of OFF and ON dominance, we measured the contrast polarity of each multiunit recording site, separately for each eye. These measurements of contrast polarity demonstrate again a pronounced bias towards OFF dominated spatial phases in layer 4 of cat visual cortex. In the cortical representation of the contralateral eye, OFF dominated phases were twice as frequent as ON dominated phases (Fig. 3, OFF: 566 vs. ON: 219) and a weaker but still robust bias could be demonstrated in the cortical representation of the ipsilateral eye (Fig. 3, OFF: 331 vs. ON: 221). This OFF bias was even more pronounced in single neurons (Supplementary Fig. 1), which were predominantly monocular in layer 4. Contrast polarity was bimodally distributed (Fig. 3 histograms, contralateral eye: $P = 0.041$; ipsilateral eye: $P < 0.001$, Hartigan tests), especially at binocular recording sites (Fig. 3 scatter plot, contralateral eye: $P = 0.0066$; ipsilateral eye: $P = 0.0015$, Hartigan tests). These bimodal distributions indicate that most layer 4 neurons have receptive fields that are either ON dominated or OFF dominated and that few neurons have receptive fields with similarly strong ON and OFF subregions. Notice that the percentage of binocular recordings was higher among neurons driven by the

ipsilateral eye because fewer monocular cells were driven by this eye (Fig. 3, top right histogram, I: 46% vs. C: 32%). Most binocular recordings were either OFF dominated by both eyes (n = 99/238, 42%) or ON dominated by one eye and OFF dominated by the other (n = 96/238, 40%). The finding that only 18% of binocular recordings were ON dominated by both eyes (Fig. 3, n = 43/238) provides further support to the notion that OFF thalamic afferents are better represented in visual cortex than ON thalamic afferents[7, 9], probably as a consequence of activity-dependent mechanisms[10].

Columnar organization for spatial phase

In theory, the visual cortex could have columns for ON/OFF dominance and no columns for ON/OFF spatial phase. For example, if the positions of the OFF-dominant subregions were randomly distributed through the depth of the cortex, the spatial phases would also be random (Fig. 1a, left). Alternatively, if the positions of the OFF-dominant subregions were maintained through the depth of the cortex, the absolute spatial phases would not change (Fig. 1a, right). Our results support the second scenario and demonstrate that the columnar organizations for ON/OFF dominance and ON/OFF absolute spatial phase are closely related. In OFF-dominated columns, the position of the OFF-dominant subregion remained constant through the depth of the cortex (OFF-phase column) and, in ON-dominated columns, the position of the ON subregion remained constant (ON-phase column). The vertical organization for spatial phase could be demonstrated with both white noise and grating stimuli. In multiunit recordings, grating stimuli were more effective at mapping multiple subregions of the receptive field (Fig. 4a) while white noise was most effective at mapping the strongest subregion (Fig. 2a). Examples of receptive fields measured with grating stimuli in multiunit recordings are shown in Figure 4a. In all examples, the spatial phase remained relatively constant through the vertical dimension but changed across different orientation columns. As predicted from the population receptive field of thalamic afferents[7] (Supplementary Fig. 2), the spatial phase was more diverse when recording from single neurons than multiunit activity. However, even among single neurons, there was clear tendency for the spatial position and polarity of the dominant receptive field subregion to remain constant through the depth of layer 4 (Fig. 4b, OFF subregion in rec 1; ON subregion in rec 2; ON subregion in rec 3). Even in cortical penetrations that showed diversity of spatial phases (rec 4–5) or a full phase shift (rec 6), neighboring cells frequently had superimposed dominant subregions of the same sign (ON subregion of top 3 cells in rec 4; OFF subregion of bottom 3 cells in rec 5; OFF subregion of top two cells and ON subregion of bottom two cells rec 6). It should be noticed that these measurements of phase variability may be overestimated by our inability to perform penetrations that are perfectly perpendicular to the cortex.

To quantify the variation in spatial phase through the depth of the cortex, we calculated the spatial correlation between receptive field pairs measured at different vertical distances within layer 4, from 0.1 mm to 0.4 mm. The spatial correlation approached a value of 1 when the receptive fields were nearly identical and −1 when they were in counter-phase. At a vertical distance of 0.1 mm, the spatial correlation calculated between receptive fields measured with multiunit activity was strongly biased towards positive values (r = 0.61) and fell as the distance increased (Fig. 4c). The spatial correlation at 0.1 mm was ~ 3 times

weaker when recording from single neurons (r = 0.26, Fig. 4d, orange lines) but it was still higher than correlations measured at 0.3 mm (r=0.1, Fig. 4d, green lines, P = 0.0074, two-sided Wilcoxon-rank-sum test) and correlations that would be expected by chance (r = 0.1, P < 0.0001, two-sided Wilcoxon-rank-sum test, see online methods). To investigate how the diversity for spatial phase compares to the diversity for orientation, we calculated the correlation between orientation tuning curves. The orientation correlation was 1 when the tuning curves were identical and −1 when they were orthogonal. The orientation correlation was high for distances of 0.1 mm (Fig. 4e–f, r = 0.95 for multiunit; r = 0.78 for single unit) and became slightly weaker as vertical distance increased, probably due to small misalignments between the axis of multielectrode and orientation column (e.g. Fig. 1b). The finding that the multiunit correlation decays faster for spatial phase than orientation indicates that orientation columns are wider than phase columns. However, since both average multiunit correlations are greater than 0.5 in a range from −1 to 1, changes in both phase and orientation are restricted to less than 1/4 cycle through the depth of layer 4.

A prediction from the receptive field arrangement of thalamic afferents to an orientation column[7] is that the average retinotopy and contrast polarity of dominant receptive field subregions should remain constant through the depth of layer 4. This prediction is supported by the examples illustrated in Figures 4a,b and by measurements of retinotopic distance between subregions dominated by the same polarity (OFF-OFF or ON-ON, Fig. 4g–h, black lines) and different polarity (ON-OFF, Fig. 4g–h, magenta lines). On average, dominant subregions with the same contrast polarity were separated by < 0.5 subregions and the separation was ~ 2 times larger for dominant subregions with different polarity, a tendency that could be demonstrated in multiunit recordings (Fig. 4g) and single neuron recordings (Fig. 4h). Therefore, while the spatial correlation between receptive field pairs was ~ 3 times higher in multiunit than single neuron recordings, the average distance between dominant subregions of the same contrast polarity was similar in both types of recordings (compare Fig. 4g and 4h). Because dominant subregions with the same contrast polarity and same position of visual space have the same absolute phase, we conclude that the columns for absolute spatial phase can be best demonstrated by measuring the spatial position of dominant ON and OFF subregions through the depth of the cortex. Receptive fields with the same absolute phase frequently differ in number of subregions, subregion strength, subregion size and position of non-dominant subregions and all these differences will reduce the values of spatial correlation. Because the variability in receptive field structure measured with white noise is less pronounced for multiunit than single neurons (e.g. compare Fig. 2a with Figure 4b), the spatial correlation should be stronger for multiunit receptive fields.

While all measurements from Figure 4 were restricted to vertical distances within 0.4 mm, the main findings could be replicated in multiunit recordings from longer vertical penetrations within layer 4 that were less orthogonal to the cortex (Fig. 5a). For example, in the recording 101 illustrated in the left panel of Figure 5a, the ON dominant subregion remained at the center of the receptive field through the depth of layer 4, slowly moving towards the right of the visual field as cortical depth increased. In recording 167 (Fig. 5a, middle), two OFF dominant subregions remained at the sides of the receptive field through the entire depth of layer 4. Finally, in recording 181 (Fig. 5a, right), an ON subregion

became increasingly stronger as cortical depth within layer 4 reached 0.3 mm while the OFF subregion retained similar strength.

Previous studies distinguished between absolute and relative phase, when comparing neighboring neurons in the cortex[2, 11]. In a columnar organization for absolute phase, the spatial position and contrast polarity of the dominant subregion do not change through the depth of layer 4 (Fig. 1a, right). In a columnar organization for relative spatial phase, the relative positions and strengths of ON and OFF subregions do not change. To distinguish between these two possible columnar organizations, we sorted all vertical penetrations with ≥ 3 contiguous receptive fields in layer 4 according to the diversity of relative spatial phases (Fig. 5b–c). For this analysis, we used all vertical electrode penetrations from layer 4, including those that were less orthogonal to the cortex, as the one illustrated in Figure 5a. The relative spatial phase was extracted from the 2-dimensional Gabor function that was best fit to the receptive fields[2] and the ON-OFF dominance was calculated by measuring the contrast polarity of the receptive field as in Figure 3 (Fig. 5b,c, black: same contrast polarity, magenta: different contrast polarity). Notice that the spatial phase can be very different in neighboring cells that are either both OFF-dominated (e.g. cells 1 and 2 in rec 1 of Fig. 4b) or both ON-dominated (e.g. cells 2 and 3 in rec 2 of Fig. 4b).

Phase diversity

Consistent with previous studies[2–6], we found a great diversity of relative spatial phases (Fig. 5b–c). However, although the relative phase changed with slight shifts in the strength and position of ON and OFF subregions, these shifts were not necessarily random (Fig. 5a). Because the diversity was smaller for absolute than relative phase (Supplementary Fig. 3), we conclude that the visual cortex has a columnar organization for absolute spatial phase and the relative phase varies more through the depth of the cortex than absolute phase. It should be noticed that the columnar organization for absolute spatial phase was restricted to layer 4 in our study. However, in occasional recordings from cortical domains strongly dominated by one contrast polarity (ON or OFF), the spatial phase could remain constant throughout more than 1 mm of cortical depth (Supplementary Fig. 4), suggesting that phase columns may extend to other cortical layers[12].

Finally, our results demonstrate that the amount of phase diversity is not the same at all columns of visual cortex but it is highest at the borders between ON- and OFF-dominated columns. Dominant receptive field subregions were ~ 2 times better overlapped in visual space when they had the same contrast polarity than when the polarity was different (Fig. 5d–e; multiunit: 67% vs. 24%, $P < 0.001$; single unit: 58% vs. 30%, $P < 0.001$, two-sided Wilcoxon-rank-sum tests). Moreover, the distribution of distances among ON and OFF dominant subregions through the depth of visual cortex (Fig. 5f–g) resembled the distribution of distances among ON and OFF receptive fields from thalamic afferents (Supplementary Fig. 5), as it would be expected if the phase columns were generated by the thalamic inputs.

DISCUSSION

Over the past decades, important advances have been made in our understanding of how spatial location and orientation are represented in primary visual cortex[13–18], however, the cortical representation of spatial phase remained unclear. This is a fundamental gap in knowledge given the importance that spatial phase has in cortical models[19–22] and image processing algorithms that are regularly applied to medicine, astronomy and telecommunication. Previous studies did not find an ordered arrangement of spatial phase when comparing neurons recorded with single electrodes[2–6]. Here, we addressed previous technical limitations by using multielectrode arrays that allowed us to record from multiple vertically aligned neurons, specifically within layer 4, where most neurons are tuned to spatial phase[23]. By doing so, we revealed a robust columnar organization for absolute spatial phase that can be demonstrated both at the level of neuronal populations and single neurons and that is likely instructed by feedforward inputs[24].

A columnar organization for spatial phase was predicted by previous computational models[17, 19–22] and our own work on the organization of thalamic afferents in visual cortex[7]. Both model[19–22] and experimental evidence[7] suggest that phase columns are likely to play a major role in the development of orientation maps. However, previous computational models frequently used limited spatial phase diversity and, therefore, they limited the neuronal resources available to process images. In the extreme, if only one spatial phase was represented in each cortical column, there would not be enough cortical space to represent a reasonable number of combinations for spatial position, phase and orientation. In contrast to previous models, the columns for spatial phase that we describe here coexist with a very diverse representation of spatial phases. The average phase of local populations of cortical neurons is preserved through the depth of the cortex but the phase is much more diverse at the level of the single neurons contributing to the average. The receptive fields of neighboring cortical neurons frequently differ in the number of subregions, subregion strength, subregion size and spatial position of the non-dominant subregions. However, they tend to have dominant subregions of the same contrast polarity in the same position of visual space. Therefore, the cortical columns for spatial phase that we describe provide a good compromise between phase diversity and phase clustering. The phase diversity could be used to accurately represent the visual scene and the phase clustering to minimize the wiring of cortical neurons that receive inputs from cells with similar phase preferences. Our results also demonstrate that the contrast polarity of the phase columns can differ between the two eyes; some orientation columns can be OFF-dominated when driven by the contralateral eye and ON-dominated when driven by the ipsilateral eye. The differences in ON/OFF dominances between eyes that we describe provide a straightforward mechanism to build maps for retinal disparity, which have been recently demonstrated in cat visual cortex[25].

An important question that remains open is whether phase columns could be demonstrated in animals without cortical orientation maps. Orientation maps are found in animals with large V1 areas such as macaques and cats but also in tree shrews. Moreover, although ferrets and rabbits have V1 areas of approximately the same size[26, 27] (144 mm^3), only ferrets have orientation maps. We notice that all animals with orientation maps have extensive binocular

visual fields and segregated eye inputs to visual cortex, either in the form of columns (e.g. macaques) or layers (e.g. tree shrews). Moreover, adding a third eye to a frog causes axonal segregation by eye input in the tectum[28], probably as a consequence of the increase in number of axons with overlapping receptive fields. Finally, while nearly all thalamic afferents with overlapping receptive fields have overlapping axon terminals in the rabbit cortex[29], thalamic afferents with overlapping receptive fields are segregated by eye input and contrast polarity in visual cortex[6, 30–32]. Based on these facts, we speculate that the position-phase visuotopy described in this paper is a consequence of the large number of thalamic afferents with overlapping receptive fields in visual cortex[7, 33, 34] and it is a unique feature of animals with orientation maps.

Online methods

Surgical preparation

Recordings from visual cortex were performed in adult male cats under general anesthesia (18 males). Cats were initially tranquilized with acepromazine (0.2mg/kg, intramuscular) and ketamine (20 mg/kg, intramuscular) and the level of anesthesia was maintained by continuous intravenous administration of propofol (3–6mg/kg/hr). Temperature, respiratory rate, indirect arterial pressure, pulse rate, expired CO_2, electrocardiogram, electroencephalogram and pulse oximetry were carefully monitored throughout the experiment. Expired carbon dioxide was maintained between 28–33 mmHg and rectal temperature between 37–38°C. Pupils were dilated with atropine sulfate (10mg per ml) and the nictitating membranes retracted with phenylephrine (20mg per ml). A topical antibiotic (gentamicin sulfate, 3 mg per ml) was administrated to prevent corneal infection. The eyes were refracted and fitted with gas-permeable contact lenses to focus on a tangent screen placed 114cm in front of the eyes. The skull and dura overlying the primary visual cortex were removed. After the surgery, animals were paralyzed with vercuronium bromide (0.24 mg/kg/hr, IV) and respired through an endotracheal tube. All procedures were performed in accordance to the guidelines of the U.S. Department of Agriculture and approved by the Institutional Animal Care and Use Committee at the State University of New York, State College of Optometry.

Electrophysiological recordings

Recorded spike waveforms were initially identified during the experiment and amplified, filtered and collected by a computer using software from Plexon (Plexon Inc, MI). A laminar array of 16 electrodes (Neuronexus, Michigan) was introduced perpendicularly into primary visual cortex to record neuronal responses (inter-electrode separation: 100 microns). The penetrations were made as orthogonal as possible to the cortical surface, however, they were not always perfectly perpendicular. Therefore, to investigate the columnar organization for spatial phase (Figure 4), we selected the penetrations in which the orientation preference changed less than 22.5 degrees through the depth of layer 4. The average orientation difference across all the electrodes within cortical layer 4 was 12.16 degrees in multiunit recording and 15.29 degrees in recordings from single neurons. We made multiple vertical penetrations with the 16-channel probe separated by 100 to 200 μm. Data for figure 2c was obtained by performing horizontal penetrations within layer 4 with a 32-channel probe with

electrode separation of 100 microns (Neuronexus). Recordings were filtered between 3 Hz and 2.2 kHz and sampled continuously at 5 kHz. Spikes from single neurons were carefully sorted with software from Plexon (Offline Sorter). To discard the possibility of recording the same isolated neuron with two different electrodes, only cell pairs with < 10% of synchronous spikes (± 1 msec) were included in our analysis. It should be noted that layer 4 neurons in cat visual cortex have dendritic fields of ~150 microns[35] and spikes are usually recorded near the most proximal dendrites. The location of cortical layer 4 was identified by current source density analysis[6, 7].

Visual stimulation and data analysis

Receptive fields were mapped with white noise[36] and gratings (Hartley stimuli)[37] by reverse correlation (stimulus update: 60 Hz). White noise was composed of a series of 32767 checkerboards (16 × 16 squares, 0.45 – 0.9° square side). The Hartley stimuli consisted of a series of 18304 stationary sinusoidal gratings with different phases, spatial frequencies and orientations (572 different gratings), each grating presented for 16.6 msec. The receptive field analysis was restricted to recordings within cortical layer 4 and receptive fields with a signal-to-noise ratio > 6. The signal-to-noise ratio was calculated as the maximum divided by the mean response at the peak frame of the receptive field. All receptive fields were normalized by the maximum response and half-rectified with a threshold of either 20% of maximum response (white noise) or 30% of maximum response (Hartley). The receptive field structure of paired recordings was compared with two different metrics: spatial correlation (*SC*) and contrast polarity (*CP*). The spatial correlation was calculated as the Pearson's correlation coefficient between the two receptive fields:

$$SC=\frac{n\cdot\sum_{i=1}^{n}x_i\cdot y_i-\sum_{i=1}^{n}x_i\cdot\sum_{i=1}^{n}y_i}{\sqrt{n\cdot\sum_{i=1}^{n}x_i^2-\left(\sum_{i=1}^{n}x_i\right)^2}\cdot\sqrt{n\cdot\sum_{i=1}^{n}y_i^2-\left(\sum_{i=1}^{n}y_i\right)^2}} \quad (1)$$

Where x_i and y_i are the normalized pixel values from the two receptive fields and n is the number of pixels in a 16 × 16 pixel matrix. *SC* equals 1 if the two receptive fields are identical and −1 if they are in counter-phase. The same Pearson's correlation coefficient was used to compare orientation tuning curves.

The contrast polarity (*CP*) was calculated as:

$$CP=\frac{\max(\mathrm{ON})-\max(\mathrm{OFF})}{\max(\mathrm{ON})+\max(\mathrm{OFF})} \quad (2)$$

Where max (ON) and max (OFF) are the maximum absolute values of ON and OFF responses. We classified all receptive fields as ON-dominated ($CP \geq 0.1$), OFF-dominated ($CP \leq -0.1$) and non-dominated ($0.1 > CP > -0.1$).

The statistical analysis for Figure 2b was performed as follows. We took 196 different vertical penetrations within layer 4 with receptive fields in contiguous electrodes that were all OFF-dominated (OFF domain), all ON-dominated (ON-domain) or mixed (ON/OFF mixed). We then assigned a value of −1 to each OFF-dominated penetration, 1 to each ON-

dominated penetration, 0 to ON/OFF mixed penetrations and created a vector with these 196 numbers. We then took randomly one number of this vector and repeated this random sampling 196 times to obtain a resampled vector. We did this procedure 1000 times to obtain 1000 resampled vectors and calculated the distributions of percentages for OFF-dominated, ON-dominated and ON/OFF mixed penetrations. The error bars in Figure 2b show the standard deviations of these distributions. Notice that the group ON/OFF mixed includes all penetrations that had at least one receptive field different from the rest (e.g. 4 OFF-dominated receptive fields and 1 ON-dominated receptive field).

To calculate the percentages that would be expected by chance, we assumed that there are twice more OFF- than ON-dominated neurons in the cortex (black bars in Figure 2b, OFF/ON = 2) or that there are equal numbers (gray bars in Figure 2b, OFF/ON = 1). The 196 vertical penetrations sampled different thicknesses of layer 4, from 0.2 mm (3 contiguous electrodes) to 0.4 mm (5 contiguous electrodes). Therefore, the percentages expected by chance were calculated by taking into account the different sample size for each layer 4 thickness (89 of 0.2 mm, 64 of 0.3 mm and 43 of 0.4 mm) and the different probabilities of finding OFF-dominated or ON-dominated neurons (OFF: ½, ON: ½ if OFF/ON = 1 and OFF: 2/3, ON: 1/3 if OFF/ON = 2). If we assume that the number of ON and OFF dominated neurons is the same (OFF/ON = 1, gray bars), the probability of finding an OFF-dominated penetration is 0.5* 0.5 * 0.5 =0.125 for 0.2 mm, 0.5 * 0.5 * 0.5 * 0.5 = 0.0625 for 0.3 mm and is 0.5 * 0.5 * 0.5 * 0.5 * 0.5 = 0.03125 for 0.4 mm, therefore, we would expect to find (0.125 * 89) + (0.0625 * 64) + (0.03125 * 43) = 16 OFF-dominated penetrations. Because we are assuming that the probability is the same for ON- than OFF-dominated neurons, we would expect to find also 16 ON-dominated penetrations and the rest should be ON/OFF mixed (196 − 16 − 16 = 164). If we assume that there are twice as many OFF-dominated than ON-dominated neurons, we would expect to find 45 OFF-dominated penetrations, $(89 * (2/3)^3) + (64 * (2/3)^4) + (43 * (2/3)^5)$; 4 ON-dominated, $(89 * (1/3)^3) + (64 * (1/3)^4) + (43 * (1/3)^5)$ and 147 ON/OFF mixed (196 − 45 − 4). The percentages expected by chance (average and standard deviations) were calculated by using the same bootstrap method described above. We created a vector of 196 numbers (e.g. 16 OFF, 16 ON and 164 ON-OFF for OFF/ON = 1), resampled this vector 1000 times and calculated the average and standard deviation of the percentages expected for OFF-dominated, ON-dominated and ON-OFF mixed penetrations. The percentages measured and expected by chance were compared also by bootstrapping. We subtracted the distributions and then calculated the ratio of values ≤ 0 relative to the total values. Because the distributions of measured percentages did not overlap the chance distributions, the ratio was 0/1000 for both distribution differences (measured vs. chance if OFF/ON = 2, measured vs. chance if OFF/ON = 1). Therefore, the probability of finding ON or OFF-dominated penetrations by chance was < 0.001.

The horizontal dimension from ON and OFF domains (Figure 2c) was calculated as follows. First, we performed horizontal penetrations through cortical layer 4 and selected the sections of these penetrations that had contiguous electrodes with ≥ 3 ON-dominated receptive fields (ON-domain) or OFF-dominated receptive fields (OFF-domain). We then counted the number of ON and OFF domains for each horizontal length (e.g. 69 OFF domains were 0.2 mm long, 40 were 0.3 mm long) and fitted the distributions for ON and OFF horizontal

length with exponential functions. To compare the decays, we created two separate vectors for ON and OFF horizontal domains. The OFF vector had 193 numbers, 69 of which had a value of 0.2 (i.e. 0.2 mm of horizontal length), 40 had a value of 0.3, 30 had a value of 0.4 and so on. The ON vector had 63 numbers, 34 of which had a value 0.2, 13 had a value of 0.3, 8 had a value 0.4 and so on. We then resampled each of the two vectors 1000 times, fitted each resampled vector with an exponential function, measured the half width at half height of the function, and obtained the distribution of the half width values. The average half-width was larger for OFF domains than ON domains (0.36 vs. 0.28 mm). To calculate the significance of this difference, we subtracted the ON and OFF distributions of half-width values and measured the ratio of values that were ≤ 0 versus the total values. Two out of 1000 values were 0 therefore the probability was $P = 0.002$.

To provide a normalized version of Figure 2c, we performed an ON/OFF-border trigger-average. First, we assigned 1 to all ON-dominated receptive fields and −1 to all OFF-dominated receptive fields within each horizontal penetration. For example, a horizontal penetration with 6 receptive fields that were OFF-OFF-OFF-OFF-ON-ON was transformed in a vector [−1 −1 −1 −1 1 1]. The vectors obtained from different horizontal penetrations were organized so that OFF domains were always before ON domains and the vectors were padded with zeros to have the ON/OFF borders aligned. For example, two vectors A = [−1 −1 −1 −1 1 1] and B = [1 1 1 −1 −1] would be transformed in A = [−1 −1 −1 −1 1 1 0] and B = [0 0 −1 −1 1 1 1]. We then averaged the vectors to obtain the final ON/OFF-border trigger-average. For example, the average of vectors A and B would be AB = [−0.5 −0.5 −1 −1 1 1 0.5]. Many of our horizontal penetrations passed through several ON and OFF domains and, therefore, they had more than one ON/OFF border. When several ON/OFF borders were present, we used the ON/OFF-border that separated the largest ON or OFF domains as the trigger of the average.

Multiunit recordings separated by 100 microns could overestimate the spatial correlation of the receptive fields if they included the same neurons. To assess the magnitude of this potential overestimate, we calculated the percentage of binocular receptive fields measured with multiunit and single unit recordings. Since ocular dominance bands in cats are ~650 microns[38] and binocular neurons in layer 4 are at the ocular dominance borders, the percentage of binocular recordings can be used to evaluate the spread of multiunit activity within cortical layer 4. The percentage of binocular recordings in layer 4 was 9% (23 out of 257) when recording from single neurons and 19% (267 out of 1416) when recording from multiunit activity (Figure 3). Therefore, if we apply these percentages to the diameter of an ocular dominance column, we sampled a cortical region of ~ 60 microns diameter when recording from single neurons (9% of 650 microns) and ~120 microns diameter when recording from multiunit activity (19% of 650). Our estimate of 120 microns diameter for the multiunit recordings is consistent with the average dendritic field of layer 4 neurons[35] (~150 microns) and previous estimates obtained from neuronal structures with much larger neurons as the hippocampus[39]. It is also consistent with our finding that multiunit recordings horizontally separated by 100 microns can have different stimulus preferences including orientation/direction, contrast polarity, spatial phase and retinotopy (data not shown). Based on these estimates, we conclude that the spatial overlap between two spheres of 120 microns

diameter separated by 100 microns (4%) is too small to cause any large overestimate of the spatial correlation measured with multiunit recordings separated by 100 microns distance. It should also be noticed that the spatial correlation between multiunit recordings separated by 300 microns was still ~8 times higher than what it would be expected by chance (r = 0.42 vs. r = 0.0556, P < 0.0001, two-sided Wilcoxon-rank-sum test). We cannot discard the possibility that some spikes from thalamic axons were included in the multiunit activity. However, it should be noticed that a main prediction being tested is that cortical phase columns are caused by the arrangement of the thalamic afferents making monosynaptic connection within the column. This phase columnar organization should be observed in recordings from multiple cortical cells including or not including thalamic afferents.

To measure the spatial correlation that would be expected by chance in Figure 4c,d, we treated all receptive fields recorded in different animals as if they were part of the same orientation column. First, we aligned all the receptive fields in visual space based on the receptive field region that generated the strongest response, which could be either ON or OFF. Then, we rotated the receptive fields so that they all had the same vertical orientation. Finally, we calculated the average spatial correlation expected by chance (r = 0.10125 for single neurons; r = 0.0556 for multiunit), which was ~ 2 times lower than the correlation measured between vertically aligned single neurons (r = 0.26 vs. r = 0.1, P < 0.0001, two-sided Wilcoxon-rank-sum test) and ~ 12 times lower than the measured correlation between vertically aligned multiunit recordings (r = 0.61 vs. 0.0556, P < 0.0001, two-sided Wilcoxon-rank-sum test).

The relative spatial phase was measured with 2D Gabor fittings[2] from receptive fields mapped with white noise. The dominant subregion was used to calculate the receptive field overlap and receptive field distance. The receptive field overlap, which ranges from 0 (no overlap) to 1 (complete overlap), was calculated with the equation:

$$\text{RF overlap} = \frac{\sum_{i=1}^{n} |x_i \cdot y_i|}{\sqrt{\sum_{i=1}^{n} x_i^2 \cdot \sum_{i=1}^{n} y_i^2}} \quad (3)$$

Where x_i and y_i are the normalized pixel values from the two receptive fields and n is the number of pixels. The receptive field distance was calculated as the distance between two dominant subregions divided by the width of the smaller subregion. Orientation was mapped with light and dark bars moving in 16 different directions (8 orientations). The orientation correlation was measured using the Pearson's correlation coefficient, as for the spatial correlation. All actual P values are reported in the manuscript except when P < 0.001. A supplementary methods checklist is available.

Supplementary Material

Refer to Web version on PubMed Central for supplementary material.

Acknowledgments

This work was supported by the US National Institutes of Health (EY005253, JMA) and DFG Research Fellowship (KR 4062/1-1, JK). We are grateful to Greg DeAngelis, Dario Ringach, Ken Miller, Ben Backus and Stewart Bloomfield for their valuable suggestions to improve this manuscript.

References

1. Woolsey TA, Van der Loos H. The structural organization of layer IV in the somatosensory region (SI) of mouse cerebral cortex. The description of a cortical field composed of discrete cytoarchitectonic units. Brain research. 1970; 17:205–242. [PubMed: 4904874]
2. DeAngelis GC, Ghose GM, Ohzawa I, Freeman RD. Functional micro-organization of primary visual cortex: receptive field analysis of nearby neurons. The Journal of neuroscience : the official journal of the Society for Neuroscience. 1999; 19:4046–4064. [PubMed: 10234033]
3. Pollen DA, Ronner SF. Phase relationships between adjacent simple cells in the visual cortex. Science. 1981; 212:1409–1411. [PubMed: 7233231]
4. Reich DS, Mechler F, Victor JD. Independent and redundant information in nearby cortical neurons. Science. 2001; 294:2566–2568. [PubMed: 11752580]
5. Yen SC, Baker J, Gray CM. Heterogeneity in the responses of adjacent neurons to natural stimuli in cat striate cortex. Journal of neurophysiology. 2007; 97:1326–1341. [PubMed: 17079343]
6. Jin JZ, et al. On and off domains of geniculate afferents in cat primary visual cortex. Nature neuroscience. 2008; 11:88–94. [PubMed: 18084287]
7. Jin J, Wang Y, Swadlow HA, Alonso JM. Population receptive fields of ON and OFF thalamic inputs to an orientation column in visual cortex. Nature neuroscience. 2011; 14:232–238. [PubMed: 21217765]
8. Das A, Gilbert CD. Distortions of visuotopic map match orientation singularities in primary visual cortex. Nature. 1997; 387:594–598. [PubMed: 9177346]
9. Yeh CI, Xing D, Shapley RM. “Black” responses dominate macaque primary visual cortex v1. The Journal of neuroscience : the official journal of the Society for Neuroscience. 2009; 29:11753–11760. [PubMed: 19776262]
10. Debanne D, Shulz DE, Fregnac Y. Activity-dependent regulation of ‘on’ and ‘off’ responses in cat visual cortical receptive fields. The Journal of physiology. 1998; 508 (Pt 2):523–548. [PubMed: 9508815]
11. Erwin E, Miller KD. Correlation-based development of ocularly matched orientation and ocular dominance maps: determination of required input activities. The Journal of neuroscience : the official journal of the Society for Neuroscience. 1998; 18:9870–9895. [PubMed: 9822745]
12. Aronov D, Reich DS, Mechler F, Victor JD. Neural coding of spatial phase in V1 of the macaque monkey. Journal of neurophysiology. 2003; 89:3304–3327. [PubMed: 12612048]
13. Blasdel GG, Salama G. Voltage-sensitive dyes reveal a modular organization in monkey striate cortex. Nature. 1986; 321:579–585. [PubMed: 3713842]
14. Bonhoeffer T, Grinvald A. Iso-orientation domains in cat visual cortex are arranged in pinwheel-like patterns. Nature. 1991; 353:429–431. [PubMed: 1896085]
15. Hubel DH, Wiesel TN. Receptive fields, binocular interaction and functional architecture in the cat’s visual cortex. The Journal of physiology. 1962; 160:106–154. [PubMed: 14449617]
16. Hubener M, Shoham D, Grinvald A, Bonhoeffer T. Spatial relationships among three columnar systems in cat area 17. The Journal of neuroscience : the official journal of the Society for Neuroscience. 1997; 17:9270–9284. [PubMed: 9364073]
17. Nauhaus I, Nielsen KJ. Building maps from maps in primary visual cortex. Current opinion in neurobiology. 2014; 24C:1–6. [PubMed: 24492071]
18. Ohki K, et al. Highly ordered arrangement of single neurons in orientation pinwheels. Nature. 2006; 442:925–928. [PubMed: 16906137]
19. Miller KD. A model for the development of simple cell receptive fields and the ordered arrangement of orientation columns through activity-dependent competition between ON- and

OFF-center inputs. The Journal of neuroscience : the official journal of the Society for Neuroscience. 1994; 14:409–441. [PubMed: 8283248]

20. Paik SB, Ringach DL. Retinal origin of orientation maps in visual cortex. Nature neuroscience. 2011; 14:919–925. [PubMed: 21623365]
21. Nakagama H, Saito T, Tanaka S. Effect of imbalance in activities between ON- and OFF-center LGN cells on orientation map formation. Biological cybernetics. 2000; 83:85–92. [PubMed: 10966048]
22. Stevens JL, Law JS, Antolik J, Bednar JA. Mechanisms for stable, robust, and adaptive development of orientation maps in the primary visual cortex. The Journal of neuroscience : the official journal of the Society for Neuroscience. 2013; 33:15747–15766. [PubMed: 24089483]
23. Martinez LM, et al. Receptive field structure varies with layer in the primary visual cortex. Nature neuroscience. 2005; 8:372–379. [PubMed: 15711543]
24. Ko H, et al. The emergence of functional microcircuits in visual cortex. Nature. 2013; 496:96–100. [PubMed: 23552948]
25. Kara P, Boyd JD. A micro-architecture for binocular disparity and ocular dominance in visual cortex. Nature. 2009; 458:627–631. [PubMed: 19158677]
26. Law MI, Zahs KR, Stryker MP. Organization of primary visual cortex (area 17) in the ferret. The Journal of comparative neurology. 1988; 278:157–180. [PubMed: 3068264]
27. Giolli RA, Pope JE. The anatomical organization of the visual system of the rabbit. Documenta ophthalmologica. Advances in ophthalmology. 1971; 30:9–31. [PubMed: 4939255]
28. Constantine-Paton M, Law MI. Eye-specific termination bands in tecta of three-eyed frogs. Science. 1978; 202:639–641. [PubMed: 309179]
29. Stoelzel CR, Bereshpolova Y, Gusev AG, Swadlow HA. The impact of an LGNd impulse on the awake visual cortex: synaptic dynamics and the sustained/transient distinction. The Journal of neuroscience : the official journal of the Society for Neuroscience. 2008; 28:5018–5028. [PubMed: 18463255]
30. Zahs KR, Stryker MP. Segregation of ON and OFF afferents to ferret visual cortex. Journal of neurophysiology. 1988; 59:1410–1429. [PubMed: 3385467]
31. Kretz R, Rager G, Norton TT. Laminar organization of ON and OFF regions and ocular dominance in the striate cortex of the tree shrew (Tupaia belangeri). The Journal of comparative neurology. 1986; 251:135–145. [PubMed: 3760256]
32. McConnell SK, LeVay S. Segregation of on- and off-center afferents in mink visual cortex. Proceedings of the National Academy of Sciences of the United States of America. 1984; 81:1590–1593. [PubMed: 6584894]
33. Martinez LM, Molano-Mazon M, Wang X, Sommer FT, Hirsch JA. Statistical wiring of thalamic receptive fields optimizes spatial sampling of the retinal image. Neuron. 2014; 81:943–956. [PubMed: 24559681]
34. Yeh CI, Stoelzel CR, Weng C, Alonso JM. Functional consequences of neuronal divergence within the retinogeniculate pathway. Journal of neurophysiology. 2009; 101:2166–2185. [PubMed: 19176606]
35. Kossel A, Lowel S, Bolz J. Relationships between dendritic fields and functional architecture in striate cortex of normal and visually deprived cats. The Journal of neuroscience : the official journal of the Society for Neuroscience. 1995; 15:3913–3926. [PubMed: 7538568]
36. Reid RC, Victor JD, Shapley RM. The use of m-sequences in the analysis of visual neurons: linear receptive field properties. Visual neuroscience. 1997; 14:1015–1027. [PubMed: 9447685]
37. Ringach DL, Sapiro G, Shapley R. A subspace reverse-correlation technique for the study of visual neurons. Vision research. 1997; 37:2455–2464. [PubMed: 9381680]
38. Anderson PA, Olavarria J, Van Sluyters RC. The overall pattern of ocular dominance bands in cat visual cortex. The Journal of neuroscience : the official journal of the Society for Neuroscience. 1988; 8:2183–2200. [PubMed: 3385494]
39. Henze DA, et al. Intracellular features predicted by extracellular recordings in the hippocampus in vivo. Journal of neurophysiology. 2000; 84:390–400. [PubMed: 10899213]

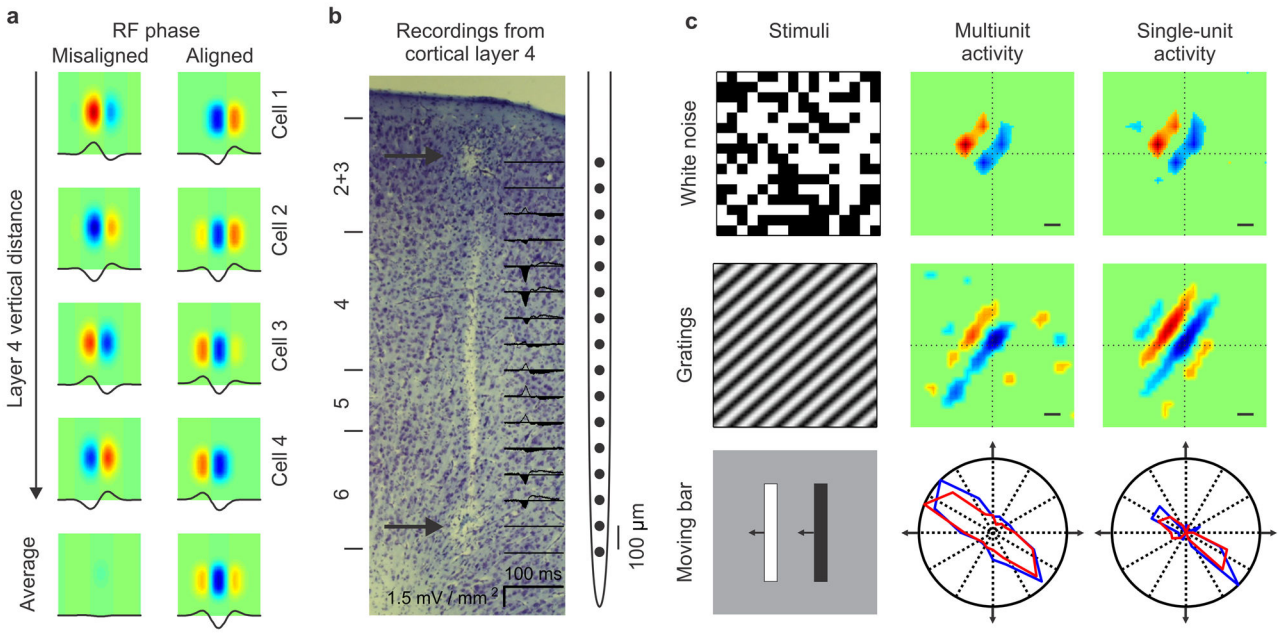

Figure 1. Measurements of receptive field structure through the depth of cortex

a. Main hypothesis. The average spatial position of ON and OFF dominant subregions is aligned through the depth of layer 4 (right panel), contrary to what is currently believed (left panel). Cell 1, 2, 3 and 4 illustrate average receptive fields of cells recorded at the 0.1, 0.2, 0.3 and 0.4 mm within the depth of layer 4. **b.** Identification of layer 4. A full-field flash generates strong current sinks in layers 4 and 6 of cat visual cortex. Two electrolytic lesions are shown at the top and bottom of the multielectrode probe (arrows). **c.** Receptive fields were mapped with white noise and gratings by reverse correlation (scale bar: 1 degree in all figures of the paper). Orientation tuning was measured with moving bars. Blue: dark; Red: light; normalized responses.

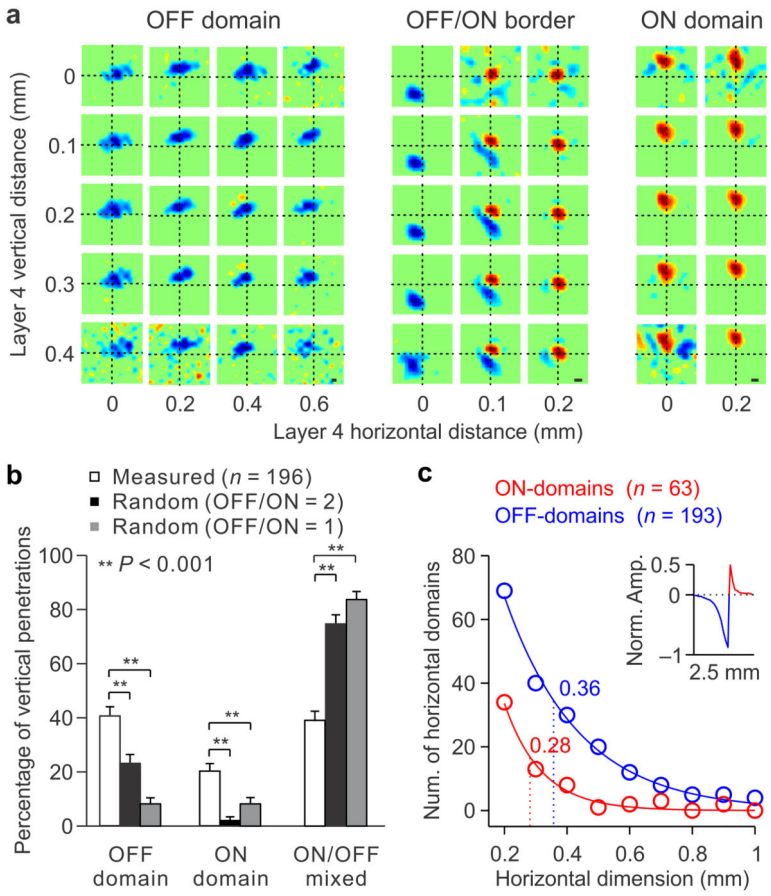

Figure 2. Columnar organization for ON and OFF dominance

a. Receptive fields measured within cortical layer 4 in an OFF domain (left), OFF/ON border (middle) and ON domain (right). Receptive fields were mapped with white noise in multiunit recordings, either simultaneously (across vertical distance) or successively (across horizontal distance). **b.** Percentage of vertical penetrations with receptive fields mapped in contiguous layer 4 electrodes that were all OFF dominated, all ON dominated or mixed (white bars). The error bars show standard deviations calculated by bootstrapping (n = 196 different vertical penetrations). The black and gray bars show the average and standard deviation of percentages expected by chance, assuming that there are twice more as many OFF-dominated than ON-dominated neurons (OFF/ON=2) or assuming equal numbers (OFF/ON=1). The measured percentages where higher than what it would be expected by chance (P < 0.001, Bootstrap, see online methods for details). **c.** Number of sections from horizontal penetrations with all receptive fields being OFF-dominated (blue) or ON-dominated (red) in three contiguous electrodes (horizontal dimension: 0.2 mm), four contiguous electrodes (horizontal dimension: 0.3 mm), and so on (see online methods for details). The dotted lines mark the horizontal spread for OFF-dominated (blue) and ON-dominated (red) domains at the half amplitude of fitted exponential functions (0.36 versus 0.28, P = 0.002, Bootstrap). The inset shows the horizontal extent of ON and OFF domains measured with ON/OFF-border trigger average (see online methods). The x axis of the inset is the same as for the main panel (horizontal dimension).

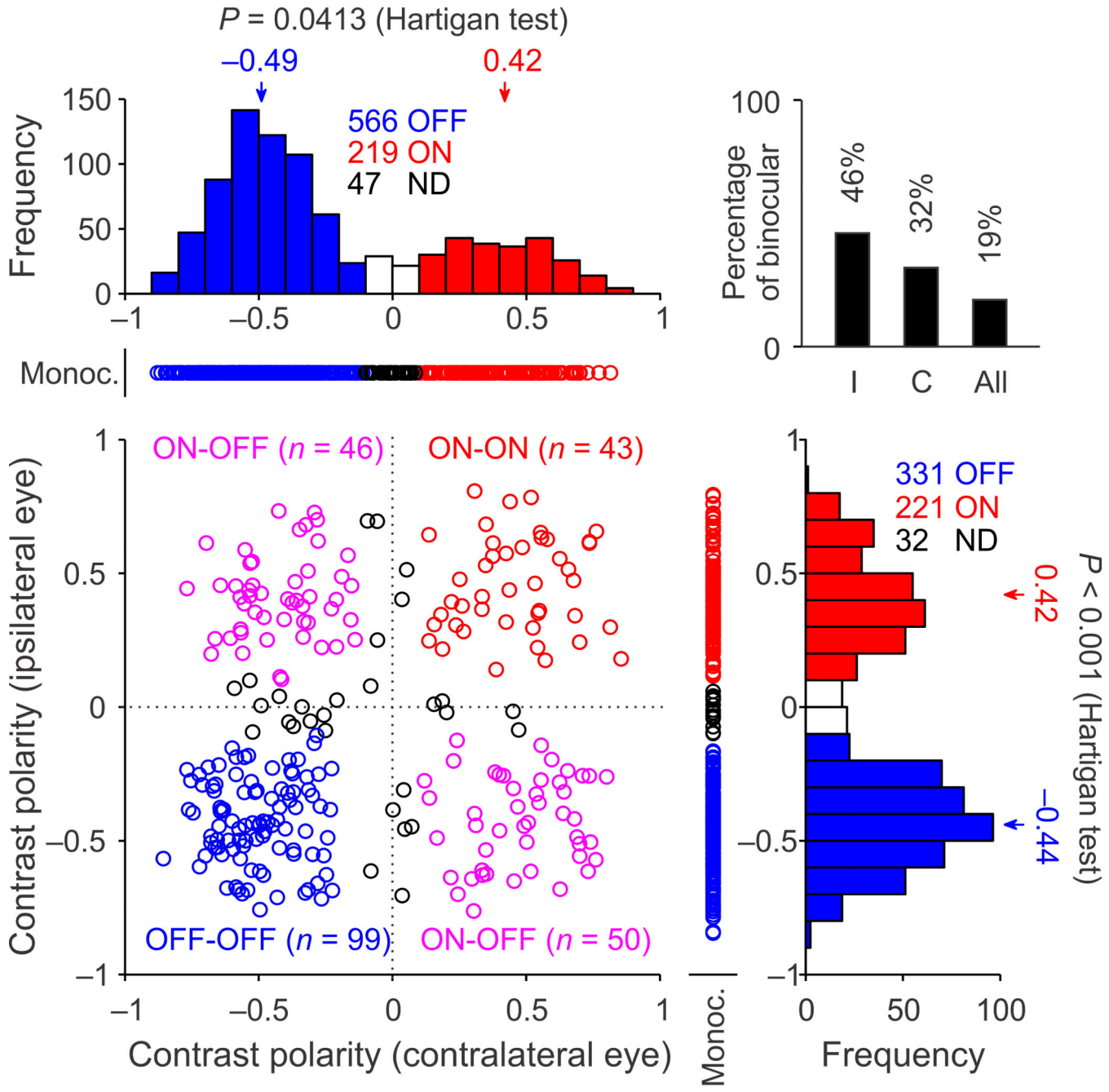

Figure 3. OFF-dominated phases are better represented in visual cortex than ON-dominated phases

Distribution of receptive-field contrast-polarity measured with white noise in multiunit recordings. Receptive fields were mapped for the contralateral eye (x axis) and ipsilateral eye (y axis). The scatter plot illustrates binocular recordings, flanked by monocular recordings (Monoc.). Red: ON-dominated. Blue: OFF-dominated. Black: non-dominated (ND). Magenta: ON-dominated by one eye and OFF-dominated by the other. The binocular receptive fields were frequently dominated by different contrast polarities for each eye (e.g. ON for contralateral eye and OFF for ipsilateral eye), however, the spatial correlation across

eyes was biased towards positive values (range: −0.17 to 0.48, mean: 0.22, median: 0.28). The histogram on the top right corner provides the number of binocular recordings (n = 267), given as a percentage of neurons driven by the contralateral eye (C, n = 832), ipsilateral eye (I, n = 584) or either eye (all, n = 1416).

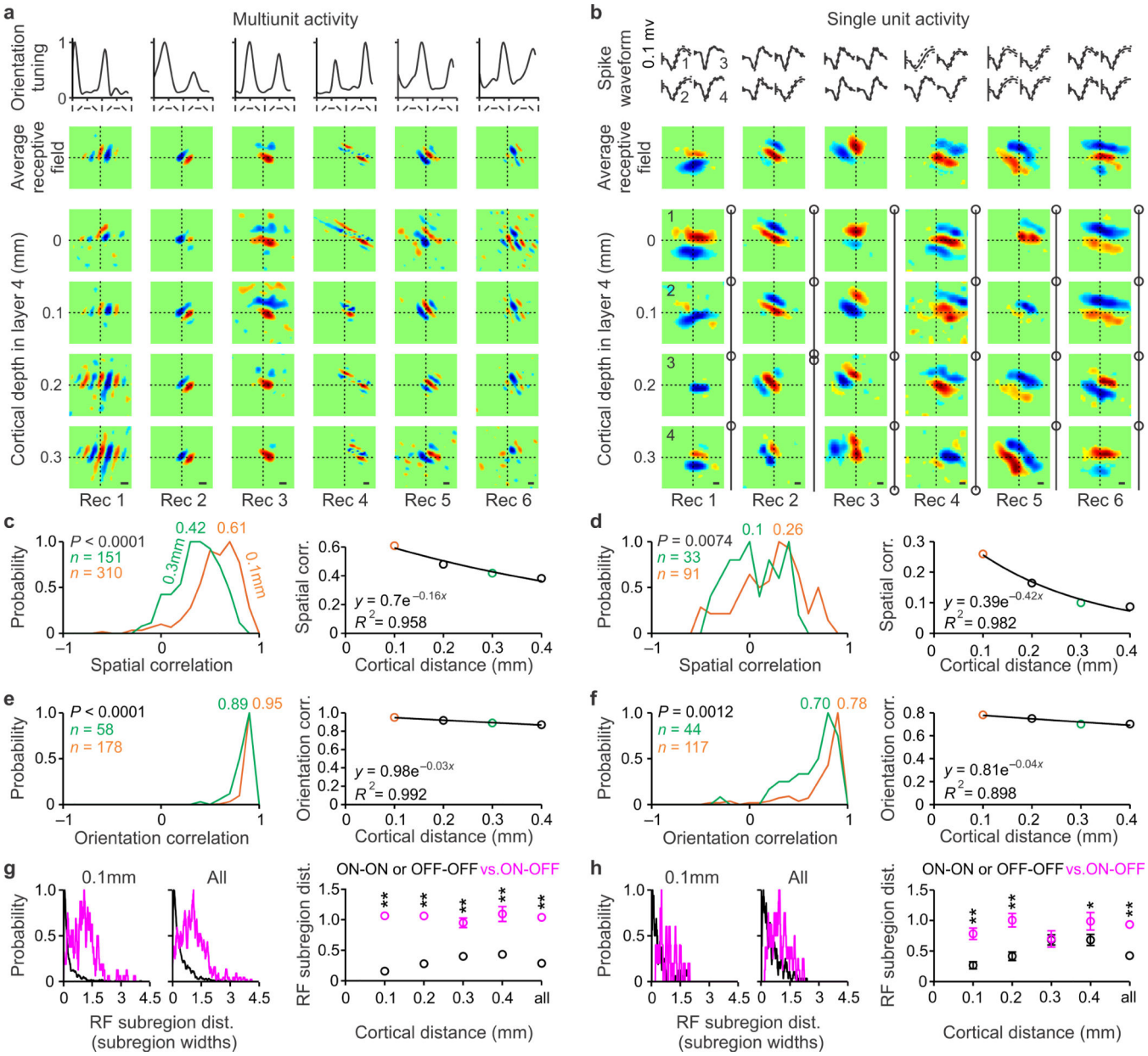

Figure 4. Columnar organization of absolute spatial phase in cat visual cortex

a. From top to bottom, orientation tuning curves, receptive field average through the depth of layer 4, and receptive fields mapped with grating stimuli at different cortical depths (multiunit activity). **b.** From top to bottom, spike waveforms from single neurons (continuous line: average; dotted line: standard deviation), receptive field average through the depth of layer 4, and receptive fields mapped with white noise at different cortical depths (single neurons). Circles show recording depth, which was the same for some neurons (e.g. recording 2). Cell pairs 1–2 in recording 2 (synchrony: 21%) and recording 6 (synchrony: 11%) where not included in the analysis of spatial phase (see online methods). **c.** Distribution of spatial correlations measured at 100 microns (orange) and 300 microns distance (green) and decay of spatial correlation with cortical distance. Probability was

calculated as the number of paired recordings for each bin normalized by the maximum bin value. **d.** Same as c for single neurons. **e–f.** Same as c–d for orientation correlation. **g.** Distance between receptive field subregions of the same (black) and different (magenta) contrast polarity at 100 microns cortical distance (left), and at all distances (middle and right). Receptive field distance was measured in units of subregion width. In the scatter plot on the right, standard errors are shown when they are larger than the diameter of the circles. **h.** Same as g for single neurons. ** $P < 0.001$ ($P < 0.0001$ except for 0.2 mm in panel h in which $P = 0.0001$), * $P = 0.0236$, $P = 0.5853$ (for 0.3 mm in panel h).

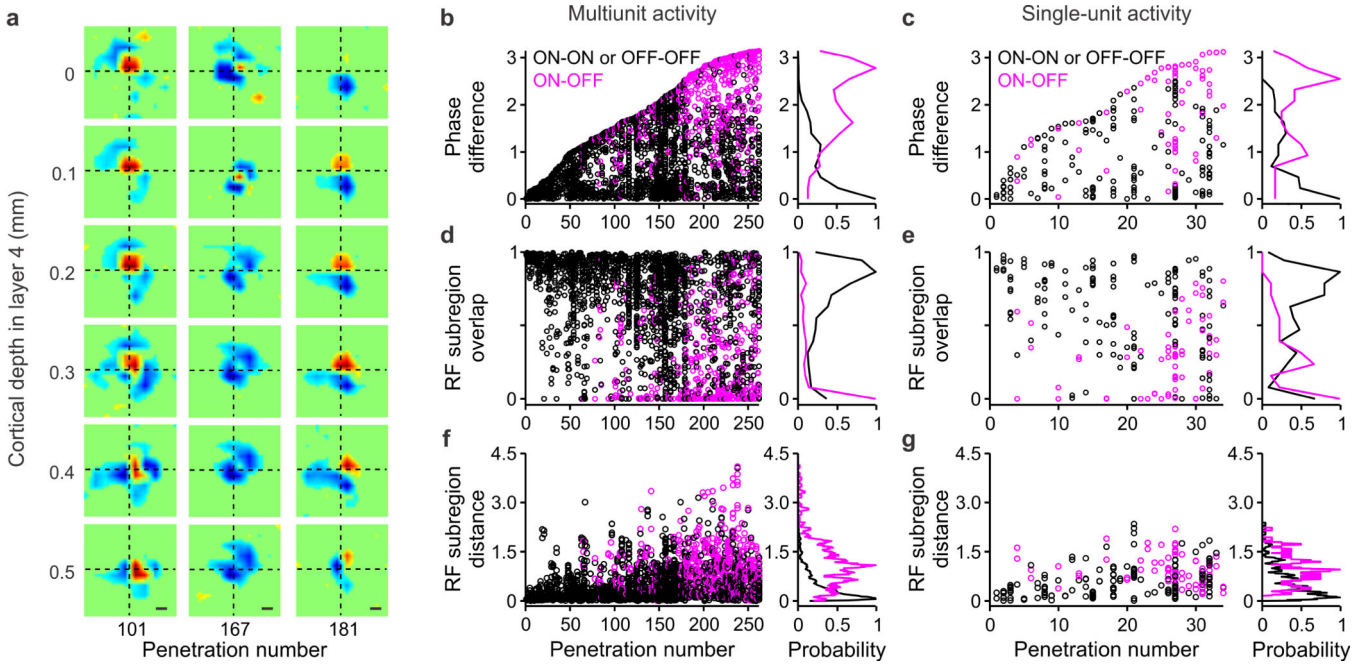

Figure 5. Diversity of relative spatial phase through the depth of layer 4

a. Example of vertical penetrations that were not perfectly orthogonal to the cortex and sampled receptive fields for distances longer than 0.4 mm within layer 4. Receptive fields were measured with white noise in multiunit recordings. The penetrations illustrate changes in average receptive field position (recording 101 on the left, recording 167 in the middle) and ON-OFF strength (recording 181 on the right) through the depth of layer 4. **b–c.** The scatter plots on the left show phase difference for each paired of receptive fields measured in each penetration, in multiunit recordings (b) and single unit recordings (c). Vertical penetrations are shown in ascending order of phase difference in the x axis, in black for receptive fields of the same contrast polarity (ON-ON or OFF-OFF) and magenta for receptive fields of the different contrast polarity (ON-OFF). The histograms on the right show the distribution of phase differences for the same contrast polarity (black) and different contrast polarity (magenta). The two distributions were significantly different ($P < 0.001$, two-sided Wilcoxon-rank-sum tests) and the same significance level was found for comparisons of distributions in panels d, e, f and g. **d–e.** Same as b–c for receptive field subregion overlap. **f–g.** Same as b–c for receptive field subregion distance (measured in units of subregion width).